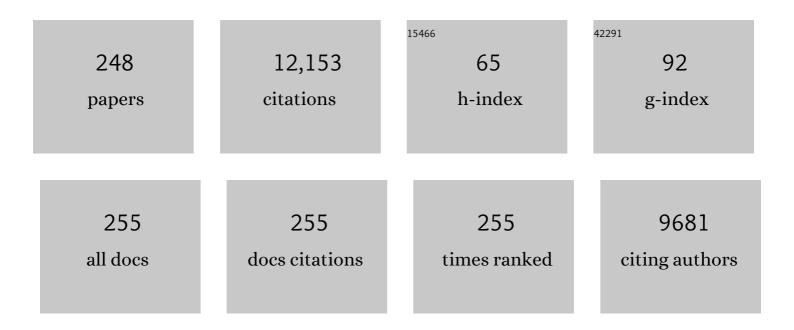
## Mohammadreza Shokouhimehr

List of Publications by Year in descending order

Source: https://exaly.com/author-pdf/7859088/publications.pdf Version: 2024-02-01



#	Article	IF	CITATIONS
1	Carbon and graphene quantum dots: a review on syntheses, characterization, biological and sensing applications for neurotransmitter determination. RSC Advances, 2020, 10, 15406-15429.	1.7	315
2	A Magnetically Recyclable Nanocomposite Catalyst for Olefin Epoxidation. Angewandte Chemie - International Edition, 2007, 46, 7039-7043.	7.2	303
3	Polymer-SupportedN-Heterocyclic Carbeneâ^Palladium Complex for Heterogeneous Suzuki Cross-Coupling Reaction. Journal of Organic Chemistry, 2005, 70, 6714-6720.	1.7	226
4	Dual purpose Prussian blue nanoparticles for cellular imaging and drug delivery: a new generation of T1-weighted MRI contrast and small molecule delivery agents. Journal of Materials Chemistry, 2010, 20, 5251.	6.7	223
5	Palladium Nanoparticles on Assorted Nanostructured Supports: Applications for Suzuki, Heck, and Sonogashira Cross-Coupling Reactions. ACS Applied Nano Materials, 2020, 3, 2070-2103.	2.4	196
6	Recent Advances in the Nanocatalyst-Assisted NaBH <sub>4</sub> Reduction of Nitroaromatics in Water. ACS Omega, 2019, 4, 483-495.	1.6	180
7	Effects of carbon additives on the properties of ZrB2–based composites: A review. Ceramics International, 2018, 44, 7334-7348.	2.3	177
8	Magnetically Separable and Sustainable Nanostructured Catalysts for Heterogeneous Reduction of Nitroaromatics. Catalysts, 2015, 5, 534-560.	1.6	171
9	Facile Aqueous-Phase Synthesis of Uniform Palladium Nanoparticles of Various Shapes and Sizes. Small, 2007, 3, 255-260.	5.2	164
10	Formation and stabilization of colloidal ultra-small palladium nanoparticles on diamine-modified Cr-MIL-101: Synergic boost to hydrogen production from formic acid. Journal of Colloid and Interface Science, 2020, 567, 126-135.	5.0	153
11	Magnetically retrievable nanocomposite adorned with Pd nanocatalysts: efficient reduction of nitroaromatics in aqueous media. Green Chemistry, 2018, 20, 3809-3817.	4.6	143
12	Performance of metal–organic frameworks in the electrochemical sensing of environmental pollutants. Journal of Materials Chemistry A, 2021, 9, 8195-8220.	5.2	135
13	Recent Advances in Applications of Voltammetric Sensors Modified with Ferrocene and Its Derivatives. ACS Omega, 2020, 5, 2049-2059.	1.6	132
14	Biocompatible Prussian blue nanoparticles: Preparation, stability, cytotoxicity, and potential use as an MRI contrast agent. Inorganic Chemistry Communication, 2010, 13, 58-61.	1.8	131
15	Recent developments in conducting polymers: applications for electrochemistry. RSC Advances, 2020, 10, 37834-37856.	1.7	131
16	Recent Developments in Polymer Nanocomposite-Based Electrochemical Sensors for Detecting Environmental Pollutants. Industrial & Engineering Chemistry Research, 2021, 60, 1112-1136.	1.8	128
17	Magnetic chitosan-copper nanocomposite: A plant assembled catalyst for the synthesis of amino- and N-sulfonyl tetrazoles in eco-friendly media. Carbohydrate Polymers, 2020, 232, 115819.	5.1	127
18	Towards artificial photosynthesis: Sustainable hydrogen utilization for photocatalytic reduction of CO2 to high-value renewable fuels. Chemical Engineering Journal, 2020, 402, 126184.	6.6	123

#	Article	IF	CITATIONS
19	Covalent Organic Frameworks: Emerging Organic Solid Materials for Energy and Electrochemical Applications. ACS Applied Materials & amp; Interfaces, 2020, 12, 27821-27852.	4.0	116
20	Novel Architecture Titanium Carbide (Ti3C2Tx) MXene Cocatalysts toward Photocatalytic Hydrogen Production: A Mini-Review. Nanomaterials, 2020, 10, 602.	1.9	114
21	Recent Electrochemical Applications of Metal–Organic Framework-Based Materials. Crystal Growth and Design, 2020, 20, 7034-7064.	1.4	112
22	Development of graphitic domains in carbon foams for high efficient electro/photo-to-thermal energy conversion phase change composites. Chemical Engineering Journal, 2019, 362, 469-481.	6.6	108
23	Microstructure and thermomechanical characteristics of spark plasma sintered TiC ceramics doped with nano-sized WC. Ceramics International, 2019, 45, 2153-2160.	2.3	107
24	Point-of-Use Rapid Detection of SARS-CoV-2: Nanotechnology-Enabled Solutions for the COVID-19 Pandemic. International Journal of Molecular Sciences, 2020, 21, 5126.	1.8	105
25	TEM characterization of spark plasma sintered ZrB2–SiC–graphene nanocomposite. Ceramics International, 2018, 44, 15269-15273.	2.3	103
26	Recent developments in palladium (nano)catalysts supported on polymers for selective and sustainable oxidation processes. Coordination Chemistry Reviews, 2019, 397, 54-75.	9.5	103
27	A screen printed electrode modified with Fe3O4@polypyrrole-Pt core-shell nanoparticles for electrochemical detection of 6-mercaptopurine and 6-thioguanine. Talanta, 2021, 232, 122379.	2.9	101
28	Magnetically recyclable hollow nanocomposite catalysts for heterogeneous reduction of nitroarenes and Suzuki reactions. Chemical Communications, 2013, 49, 4779.	2.2	100
29	Spark plasma sintering of TiN ceramics codoped with SiC and CNT. Ceramics International, 2019, 45, 3207-3216.	2.3	99
30	High performance of screen-printed graphite electrode modified with Ni–Mo-MOF for voltammetric determination of amaranth. Journal of Food Measurement and Characterization, 2021, 15, 4617-4622.	1.6	99
31	Spark plasma sintering of Al-doped ZrB2–SiC composite. Ceramics International, 2019, 45, 4262-4267.	2.3	97
32	MXenes: Applications in electrocatalytic, photocatalytic hydrogen evolution reaction and CO2 reduction. Molecular Catalysis, 2020, 486, 110850.	1.0	97
33	Nanomaterials modified electrodes for electrochemical detection of Sudan I in food. Journal of Food Measurement and Characterization, 2021, 15, 3837-3852.	1.6	95
34	Synergistic advanced oxidation process for the fast degradation of ciprofloxacin antibiotics using a GO/CuMOF-magnetic ternary nanocomposite. Journal of Environmental Chemical Engineering, 2021, 9, 105486.	3.3	95
35	Copper oxide–graphene oxide nanocomposite: efficient catalyst for hydrogenation of nitroaromatics in water. Nano Convergence, 2019, 6, 6.	6.3	94
36	Developments and applications of nanomaterial-based carbon paste electrodes. RSC Advances, 2020, 10, 21561-21581.	1.7	94

#	Article	IF	CITATIONS
37	Temperature dependence of microstructure evolution during hot pressing of ZrB2–30 vol.% SiC composites. International Journal of Refractory Metals and Hard Materials, 2016, 54, 7-13.	1.7	90
38	Palladium Nanocatalysts on Hydroxyapatite: Green Oxidation of Alcohols and Reduction of Nitroarenes in Water. Applied Sciences (Switzerland), 2019, 9, 4183.	1.3	88
39	Synthesis of bimetallic 4-PySI-Pd@Cu(BDC) via open metal site Cu-MOF: Effect of metal and support of Pd@Cu-MOFs in H2 generation from formic acid. Molecular Catalysis, 2019, 467, 30-37.	1.0	88
40	A numerical approach to the heat transfer in monolithic and SiC reinforced HfB2, ZrB2 and TiB2 ceramic cutting tools. Ceramics International, 2019, 45, 15892-15897.	2.3	86
41	Nanoindentation and nanostructural characterization of ZrB2–SiC composite doped with graphite nano-flakes. Composites Part B: Engineering, 2019, 175, 107153.	5.9	84
42	Perovskite oxide-based photocatalysts for solar-driven hydrogen production: Progress and perspectives. Solar Energy, 2020, 211, 584-599.	2.9	84
43	A Magnetically Recyclable Nanocomposite Catalyst for Olefin Epoxidation. Angewandte Chemie, 2007, 119, 7169-7173.	1.6	82
44	A novel ZrB2–VB2–ZrC composite fabricated by reactive spark plasma sintering. Materials Science & Engineering A: Structural Materials: Properties, Microstructure and Processing, 2018, 731, 131-139.	2.6	82
45	Influence of vanadium content on the characteristics of spark plasma sintered ZrB2–SiC–V composites. Journal of Alloys and Compounds, 2019, 805, 725-732.	2.8	81
46	Pd nanocatalyst stabilized on amine-modified zeolite: Antibacterial and catalytic activities for environmental pollution remediation in aqueous medium. Separation and Purification Technology, 2020, 239, 116542.	3.9	81
47	Heat transfer, thermal stress and failure analyses in a TiB2 gas turbine stator blade. Ceramics International, 2019, 45, 19331-19339.	2.3	80
48	Mainstream avenues for boosting graphitic carbon nitride efficiency: towards enhanced solar light-driven photocatalytic hydrogen production and environmental remediation. Journal of Materials Chemistry A, 2020, 8, 10571-10603.	5.2	80
49	Extended Metal–Organic Frameworks on Diverse Supports as Electrode Nanomaterials for Electrochemical Energy Storage. ACS Applied Nano Materials, 2020, 3, 3964-3990.	2.4	80
50	Polymer-Coated NH <sub>2</sub> -UiO-66 for the Codelivery of DOX/pCRISPR. ACS Applied Materials & Interfaces, 2021, 13, 10796-10811.	4.0	80
51	The emerging covalent organic frameworks (COFs) for solar-driven fuels production. Coordination Chemistry Reviews, 2021, 446, 214117.	9.5	79
52	Layerâ€Wise Titania Growth Within Dimeric Organic Functional Group Viologen Periodic Mesoporous Organosilica as Efficient Photocatalyst for Oxidative Formic Acid Decomposition. ChemCatChem, 2019, 11, 4803-4809.	1.8	78
53	Photocatalytic NOx abatement: Recent advances and emerging trends in the development of photocatalysts. Journal of Cleaner Production, 2020, 270, 121912.	4.6	78
54	Twoâ€Dimensional Metal–Organic Frameworks and Covalent–Organic Frameworks for Electrocatalysis: Distinct Merits by the Reduced Dimension. Advanced Energy Materials, 2022, 12, 2003990.	10.2	78

#	Article	IF	CITATIONS
55	Natural Polymers Decorated MOF-MXene Nanocarriers for Co-delivery of Doxorubicin/pCRISPR. ACS Applied Bio Materials, 2021, 4, 5106-5121.	2.3	78
56	A numerical approach to the heat transfer and thermal stress in a gas turbine stator blade made of HfB2. Ceramics International, 2019, 45, 24060-24069.	2.3	77
57	Numerical analyses of heat transfer and thermal stress in a ZrB2 gas turbine stator blade. Ceramics International, 2019, 45, 17742-17750.	2.3	77
58	Palladium nanoparticles stabilized on a novel Schiff base modified Unye bentonite: Highly stable, reusable and efficient nanocatalyst for treating wastewater contaminants and inactivating pathogenic microbes. Separation and Purification Technology, 2020, 237, 116383.	3.9	76
59	Facile synthesis of monodispersed Pd nanocatalysts decorated on graphene oxide for reduction of nitroaromatics in aqueous solution. Research on Chemical Intermediates, 2019, 45, 599-611.	1.3	75
60	Magnetically separable carbon nanocomposite catalysts for efficient nitroarene reduction and Suzuki reactions. Applied Catalysis A: General, 2014, 476, 133-139.	2.2	73
61	Boosting Aerobic Oxidation of Alcohols via Synergistic Effect between TEMPO and a Composite Fe <sub>3</sub> O <sub>4</sub> /Cu-BDC/GO Nanocatalyst. ACS Omega, 2020, 5, 5182-5191.	1.6	73
62	The effect of thermal contact resistance on the temperature distribution in a WC made cutting tool. Ceramics International, 2019, 45, 22196-22202.	2.3	72
63	Synergetic effects of SiC and Csf in ZrB2-based ceramic composites. Part I: Densification behavior. Ceramics International, 2016, 42, 4498-4506.	2.3	71
64	Effects of graphite nano-flakes on thermal and microstructural properties of TiB2–SiC composites. Ceramics International, 2020, 46, 11622-11630.	2.3	71
65	Magnetically recyclable core–shell nanocatalysts for efficient heterogeneous oxidation of alcohols. Journal of Materials Chemistry A, 2014, 2, 7593-7599.	5.2	67
66	Recent advances in <i>N</i> -formylation of amines and nitroarenes using efficient (nano)catalysts in eco-friendly media. Green Chemistry, 2019, 21, 5144-5167.	4.6	67
67	Investigation of hot pressed ZrB2–SiC–carbon black nanocomposite by scanning and transmission electron microscopy. Ceramics International, 2019, 45, 16759-16764.	2.3	66
68	Electron microscopy investigation of spark plasma sintered ZrO2 added ZrB2–SiC composite. Ceramics International, 2020, 46, 19646-19649.	2.3	66
69	Green metal-organic frameworks (MOFs) for biomedical applications. Microporous and Mesoporous Materials, 2022, 335, 111670.	2.2	65
70	SnS <sub>2</sub> Nanograins on Porous SiO <sub>2</sub> Nanorods Template for Highly Sensitive NO <sub>2</sub> Sensor at Room Temperature with Excellent Recovery. ACS Sensors, 2019, 4, 678-686.	4.0	64
71	Palladium Nanocatalysts Confined in Mesoporous Silica for Heterogeneous Reduction of Nitroaromatics. Energy and Environment Focus, 2015, 4, 18-23.	0.3	64
72	Electrocatalytic Water Splitting and CO <sub>2</sub> Reduction: Sustainable Solutions via Singleâ€Atom Catalysts Supported on 2D Materials. Small Methods, 2019, 3, 1800492.	4.6	63

#	Article	IF	CITATIONS
73	Palladium Comprising Dicationic Bipyridinium Supported Periodic Mesoporous Organosilica (PMO): Pd@Bipy–PMO as an Efficient Hybrid Catalyst for Suzuki–Miyaura Cross-Coupling Reaction in Water. Catalysts, 2019, 9, 140.	1.6	63
74	Facile synthesis of graphitic carbon nitride/chitosan/Au nanocomposite: A catalyst for electrochemical hydrogen evolution. International Journal of Biological Macromolecules, 2020, 164, 3012-3024.	3.6	62
75	Numerical modeling of heat transfer during spark plasma sintering of titanium carbide. Ceramics International, 2020, 46, 7615-7624.	2.3	59
76	In situ preparation of g-C3N4 nanosheet/FeOCI: Achievement and promoted photocatalytic nitrogen fixation activity. Journal of Colloid and Interface Science, 2021, 587, 538-549.	5.0	59
77	Organofacies study of the Bakken source rock in North Dakota, USA, based on organic petrology and geochemistry. International Journal of Coal Geology, 2018, 188, 79-93.	1.9	58
78	Recent Advances in Rechargeable Aluminum-Ion Batteries and Considerations for Their Future Progress. ACS Applied Energy Materials, 2020, 3, 6019-6035.	2.5	58
79	Influence of SiAlON addition on the microstructure development of hot-pressed ZrB2–SiC composites. Ceramics International, 2020, 46, 19209-19216.	2.3	58
80	Turning Toxic Nanomaterials into a Safe and Bioactive Nanocarrier for Co-delivery of DOX/pCRISPR. ACS Applied Bio Materials, 2021, 4, 5336-5351.	2.3	57
81	Densification behavior and microstructure development in TiB2 ceramics doped with h-BN. Ceramics International, 2020, 46, 18970-18975.	2.3	56
82	Heterogeneous Suzuki Cross-Coupling Reaction Catalyzed by Magnetically Recyclable Nanocatalyst. Bulletin of the Korean Chemical Society, 2013, 34, 1477-1480.	1.0	56
83	Recent developments in electrochemical sensors for detecting hydrazine with different modified electrodes. RSC Advances, 2020, 10, 30481-30498.	1.7	55
84	+Iron hexacyanocobaltate metal-organic framework: Highly reversible and stationary electrode material with rich borders for lithium-ion batteries. Journal of Alloys and Compounds, 2019, 791, 911-917.	2.8	54
85	Novel p–n Heterojunction Nanocomposite: TiO <sub>2</sub> QDs/ZnBi <sub>2</sub> O <sub>4</sub> Photocatalyst with Considerably Enhanced Photocatalytic Activity under Visible-Light Irradiation. Journal of Physical Chemistry C, 2020, 124, 27519-27528.	1.5	54
86	One-pot synthesis of magnetically recyclable mesoporous silica supported acid–base catalysts for tandem reactions. Chemical Communications, 2013, 49, 7821.	2.2	53
87	Visible-light-driven photocatalytic activity of ZnO/g-C3N4 heterojunction for the green synthesis of biologically interest small molecules of thiazolidinones. Journal of Photochemistry and Photobiology A: Chemistry, 2020, 402, 112786.	2.0	52
88	Pd- and Au-Decorated MoS2 Gas Sensors for Enhanced Selectivity. Electronic Materials Letters, 2019, 15, 368-376.	1.0	50
89	Recent Advances in Electrochemical Sensors and Biosensors for Detecting Bisphenol A. Sensors, 2020, 20, 3364.	2.1	50
90	Role of nano-diamond addition on the characteristics of spark plasma sintered TiC ceramics. Diamond and Related Materials, 2020, 106, 107828.	1.8	49

#	Article	IF	CITATIONS
91	Characterization of spark plasma sintered TiC ceramics reinforced with graphene nano-platelets. Ceramics International, 2020, 46, 18742-18749.	2.3	48
92	Heat transfer and pressure drop in a ZrB2 microchannel heat sink: A numerical approach. Ceramics International, 2020, 46, 1730-1735.	2.3	45
93	Microstructural and mechanical characterization of spark plasma sintered TiC ceramics with TiN additive. Ceramics International, 2020, 46, 18924-18932.	2.3	45
94	Two-dimensional boron nitride as a sulfur fixer for high performance rechargeable aluminum-sulfur batteries. Scientific Reports, 2019, 9, 13573.	1.6	44
95	Correlating Rock-Evalâ,,¢ Tmax with bitumen reflectance from organic petrology in the Bakken Formation. International Journal of Coal Geology, 2019, 205, 87-104.	1.9	44
96	Enhanced fracture toughness of ZrB2–SiCw ceramics with graphene nano-platelets. Ceramics International, 2020, 46, 24906-24915.	2.3	43
97	Multifunctional 3D Hierarchical Bioactive Green Carbon-Based Nanocomposites. ACS Sustainable Chemistry and Engineering, 2021, 9, 8706-8720.	3.2	43
98	Modulated large-pore mesoporous silica as an efficient base catalyst for the Henry reaction. Research on Chemical Intermediates, 2018, 44, 1617-1626.	1.3	42
99	Nanomaterials for modulating innate immune cells in cancer immunotherapy. Asian Journal of Pharmaceutical Sciences, 2019, 14, 16-29.	4.3	41
100	Synthesis of 1-Substituted 1 <i>H</i> -1,2,3,4-Tetrazoles Using Biosynthesized Ag/Sodium Borosilicate Nanocomposite. ACS Omega, 2019, 4, 8985-9000.	1.6	38
101	Numerical simulation of heat transfer during spark plasma sintering of zirconium diboride. Ceramics International, 2020, 46, 4998-5007.	2.3	38
102	Nanoindentational and conventional mechanical properties of spark plasma sintered Ti–Mo alloys. Journal of Materials Research and Technology, 2020, 9, 10647-10658.	2.6	36
103	Characteristics of quadruplet Ti–Mo–TiB2–TiC composites prepared by spark plasma sintering. Ceramics International, 2020, 46, 20885-20895.	2.3	36
104	Combustion synthesized YVO4:Eu3+ phosphors: Effect of fuels on nanostructure and luminescence properties. Ceramics International, 2017, 43, 11469-11473.	2.3	35
105	Nanomaterials for bone tissue regeneration: updates and future perspectives. Nanomedicine, 2019, 14, 2987-3006.	1.7	35
106	Effects of SiC content on thermal shock behavior and elastic modulus of cordierite–mullite composites. Ceramics International, 2020, 46, 23780-23784.	2.3	35
107	Beneficial role of carbon black on the properties of TiC ceramics. Ceramics International, 2020, 46, 23544-23555.	2.3	35
108	Electrochemical Detection of Hydrazine by Carbon Paste Electrode Modified with Ferrocene Derivatives, Ionic Liquid, and CoS <sub>2</sub> -Carbon Nanotube Nanocomposite. ACS Omega, 2021, 6, 4641-4648.	1.6	35

#	Article	IF	CITATIONS
109	Gadolinium Triflate Immobilized on Magnetic Nanocomposites as Recyclable Lewis Acid Catalyst for Acetylation of Phenols. Nanoscience and Nanotechnology Letters, 2014, 6, 309-313.	0.4	35
110	Improved photocatalytic activity of ZnO-TiO <sub>2</sub> nanocomposite catalysts by modulating TiO <sub>2</sub> thickness. Materials Research Express, 2019, 6, 115060.	0.8	34
111	Adsorption mechanism of a cationic dye on a biomass-derived micro- and mesoporous carbon: structural, kinetic, and equilibrium insight. Biomass Conversion and Biorefinery, 2021, 11, 943-954.	2.9	34
112	Properties of CoS2/CNT as a Cathode Material of Rechargeable Aluminum-Ion Batteries. Electronic Materials Letters, 2019, 15, 727-732.	1.0	33
113	Understanding organic matter heterogeneity and maturation rate by Raman spectroscopy. International Journal of Coal Geology, 2019, 206, 46-64.	1.9	33
114	Enhanced densification of spark plasma sintered TiB2 ceramics with low content AlN additive. Ceramics International, 2020, 46, 22127-22133.	2.3	33
115	Recent development of high-performance photocatalysts for N2 fixation: A review. Journal of Environmental Chemical Engineering, 2021, 9, 104997.	3.3	33
116	Layered metal–organic framework based on tetracyanonickelate as a cathode material for <i>in situ</i> Li-ion storage. RSC Advances, 2019, 9, 21363-21370.	1.7	32
117	Facile synthesis and electrochemical hydrogen storage of bentonite/TiO2/Au nanocomposite. International Journal of Hydrogen Energy, 2020, 45, 33771-33788.	3.8	32
118	Role of co-addition of BN and SiC on microstructure of TiB2-based composites densified by SPS method. Ceramics International, 2020, 46, 25341-25350.	2.3	32
119	Synthesis of <scp> MoS <sub>x</sub> </scp> /Niâ€metalâ€organic frameworkâ€74 composites as efficient electrocatalysts for hydrogen evolution reactions. International Journal of Energy Research, 2021, 45, 9638-9647.	2.2	32
120	Metal-free nanostructured catalysts: sustainable driving forces for organic transformations. Green Chemistry, 2021, 23, 6223-6272.	4.6	32
121	High-impressive separation of photoinduced charge carriers on step-scheme ZnO/ZnSnO3/Carbon dots heterojunction with efficient activity in photocatalytic NH3 production. Journal of the Taiwan Institute of Chemical Engineers, 2021, 118, 140-151.	2.7	32
122	Recent developments in voltammetric and amperometric sensors for cysteine detection. RSC Advances, 2021, 11, 5411-5425.	1.7	32
123	Pd nanoparticles loaded on modified chitosan-Unye bentonite microcapsules: A reusable nanocatalyst for Sonogashira coupling reaction. Carbohydrate Polymers, 2021, 262, 117920.	5.1	32
124	Metal Hexacyanoferrate Nanoparticles as Electrode Materials for Lithium Ion Batteries. Nanoscience and Nanotechnology Letters, 2013, 5, 770-774.	0.4	32
125	Enhanced visible photocatalytic degradation of diclofen over N-doped TiO2 assisted with H2O2: A kinetic and pathway study. Arabian Journal of Chemistry, 2020, 13, 8361-8371.	2.3	31
126	Electron microscopy characterization of porous ZrB2–SiC–AlN composites prepared by pressureless sintering. Ceramics International, 2020, 46, 25415-25423.	2.3	30

#	Article	IF	CITATIONS
127	Recent Advances in the Aptamer-Based Electrochemical Biosensors for Detecting Aflatoxin B1 and Its Pertinent Metabolite Aflatoxin M1. Sensors, 2020, 20, 3256.	2.1	30
128	Physical, mechanical and microstructural characterization of TiC–ZrN ceramics. Ceramics International, 2020, 46, 22154-22163.	2.3	30
129	Edge-exposed WS2 on 1D nanostructures for highly selective NO2 sensor at room temperature. Sensors and Actuators B: Chemical, 2021, 333, 129566.	4.0	30
130	Green chemistry and coronavirus. Sustainable Chemistry and Pharmacy, 2021, 21, 100415.	1.6	29
131	Photocatalytic hydrogen generation using colloidal covalent organic polymers decorated bimetallic Au-Pd nanoalloy (COPs/Pd-Au). Molecular Catalysis, 2022, 518, 112058.	1.0	29
132	Realization of Lithium-Ion Capacitors with Enhanced Energy Density via the Use of Gadolinium Hexacyanocobaltate as a Cathode Material. ACS Applied Materials & Interfaces, 2019, 11, 31799-31805.	4.0	28
133	Coordinating gallium hexacyanocobaltate: Prussian blue-based nanomaterial for Li-ion storage. RSC Advances, 2019, 9, 26668-26675.	1.7	28
134	Metal-organic framework-derived metal oxide nanoparticles@reduced graphene oxide composites as cathode materials for rechargeable aluminium-ion batteries. Scientific Reports, 2019, 9, 13739.	1.6	28
135	A Hybrid Energy Storage Mechanism of Zinc Hexacyanocobaltate-Based Metal–Organic Framework Endowing Stationary and High-Performance Lithium-Ion Storage. Electronic Materials Letters, 2019, 15, 444-453.	1.0	28
136	The Pschorr Reaction, a Fresh Look at a Classical Transformation. Current Organic Synthesis, 2009, 6, 193-202.	0.7	27
137	Graphene derivatives supported nanocatalysts for oxygen reduction reaction. Chinese Journal of Catalysis, 2015, 36, 1799-1810.	6.9	27
138	MOF-derived NiFe2O4 nanoparticles on molybdenum disulfide: Magnetically reusable nanocatalyst for the reduction of nitroaromatics in aqueous media. Journal of Industrial and Engineering Chemistry, 2022, 107, 428-435.	2.9	27
139	Light-directed synthesis of peptide nucleic acids (PNAs) chips. Biosensors and Bioelectronics, 2007, 22, 2891-2897.	5.3	26
140	Three-dimensionally interconnected porous boron nitride foam derived from polymeric foams. RSC Advances, 2016, 6, 51426-51434.	1.7	26
141	Comprehensive Study on the Morphology Control of TiO <sub>2</sub> Nanorods on Foreign Substrates by the Hydrothermal Method. Crystal Growth and Design, 2018, 18, 6504-6512.	1.4	26
142	Influence of Ni/Co binders and Mo2C on the microstructure evolution and mechanical properties of (Ti0.93W0.07)C–based cermets. Ceramics International, 2018, 44, 17655-17659.	2.3	26
143	The Combustion Synthesis of Ag-Doped MnCo2O4 Nanoparticles for Supercapacitor Applications. Jom, 2019, 71, 1499-1506.	0.9	26
144	Role of hot-pressing temperature on densification and microstructure of ZrB2–SiC ultrahigh temperature ceramics. International Journal of Refractory Metals and Hard Materials, 2020, 93, 105355.	1.7	26

#	Article	IF	CITATIONS
145	Pd modified prussian blue frameworks: Multiple electron transfer pathways for improving catalytic activity toward hydrogenation of nitroaromatics. Molecular Catalysis, 2020, 492, 110967.	1.0	26
146	Synthesis of mesoporous tungsten oxide by template-assisted sol–gel method and its photocatalytic degradation activity. Journal of Sol-Gel Science and Technology, 2017, 82, 148-156.	1.1	25
147	A novel TiC-based composite co-strengthened with AlN particulates and graphene nano-platelets. International Journal of Refractory Metals and Hard Materials, 2020, 92, 105331.	1.7	25
148	Structural Evolution of Organic Matter in Deep Shales by Spectroscopy ( <sup>1</sup> H and) Tj ETQq0 0 0 rgBT	Overlock 2.5	10 Tf 50 627 25
149	Comparison of fractal dimensions from nitrogen adsorption data in shale <i>via</i> different models. RSC Advances, 2021, 11, 2298-2306.	1.7	25
150	Molecular weight variations of kerogen during maturation with MALDI-TOF-MS. Fuel, 2020, 269, 117452.	3.4	25
151	High gravity-assisted green synthesis of ZnO nanoparticles via Allium ursinum: Conjoining nanochemistry to neuroscience. Nano Express, 2020, 1, 020025.	1.2	25
152	Simple Synthesis of Twoâ€Ðimensional Micro/Mesoporous Boron Nitride. European Journal of Inorganic Chemistry, 2015, 2015, 2478-2485.	1.0	24
153	Prussian blue-based nanostructured materials: Catalytic applications for environmental remediation and energy conversion. Molecular Catalysis, 2021, 514, 111835.	1.0	24
154	Novel production of natural bacteriocin via internalization of dextran nanoparticles into probiotics. Biomaterials, 2019, 218, 119360.	5.7	23
155	S@GO as a High-Performance Cathode Material for Rechargeable Aluminum-Ion Batteries. Electronic Materials Letters, 2019, 15, 720-726.	1.0	23
156	Graphite carbon-encapsulated metal nanoparticles derived from Prussian blue analogs growing on natural loofa as cathode materials for rechargeable aluminum-ion batteries. Scientific Reports, 2019, 9, 13665.	1.6	23
157	Cerium Hexacyanocobaltate: A Lanthanide-Compliant Prussian Blue Analogue for Li-Ion Storage. ACS Omega, 2019, 4, 21410-21416.	1.6	23
158	A Screen-Printed Electrode Modified With Graphene/Co3O4 Nanocomposite for Electrochemical Detection of Tramadol. Frontiers in Chemistry, 2020, 8, 562308.	1.8	23
159	Curbed of molybdenum oxido-diperoxido complex on ionic liquid body of mesoporous Bipy-PMO-IL as a promising catalyst for selective sulfide oxidation. Journal of Molecular Liquids, 2020, 312, 113388.	2.3	23
160	Chemical heterogeneity of organic matter at nanoscale by AFM-based IR spectroscopy. Fuel, 2020, 261, 116454.	3.4	22
161	Microstructural, mechanical and friction properties of nano-graphite and h-BN added TiC-based composites. Ceramics International, 2020, 46, 28969-28979.	2.3	22
162	3D Bioprinted Bacteriostatic Hyperelastic Bone Scaffold for Damage-Specific Bone Regeneration. Polymers, 2021, 13, 1099.	2.0	22

#	Article	IF	CITATIONS
163	One pot synthesis of mesoporous boron nitride using polystyrene-b-poly(ethylene oxide) block copolymer. RSC Advances, 2015, 5, 6528-6535.	1.7	21
164	Tailorable Topologies for Selectively Controlling Crystals of Expanded Prussian Blue Analogues. Crystal Growth and Design, 2019, 19, 7385-7395.	1.4	21
165	Impact of process parameters on luminescence properties and nanostructure of YVO4:Eu phosphor. Materials Chemistry and Physics, 2019, 229, 431-436.	2.0	21
166	Insight into the Self-Insertion of a Protein Inside the Boron Nitride Nanotube. ACS Omega, 2020, 5, 32051-32058.	1.6	21
167	Boron nitride-palladium nanostructured catalyst: efficient reduction of nitrobenzene derivatives in water. Nano Express, 2020, 1, 030012.	1.2	21
168	Facile synthesis of nanostructured carbon nanotube/iron oxide hybrids for lithium-ion battery anodes. RSC Advances, 2014, 4, 37365-37370.	1.7	20
169	Two-dimensional assemblies of ultrathin titanate nanosheets for lithium ion battery anodes. RSC Advances, 2014, 4, 12087.	1.7	20
170	Characteristics of dynamically formed oxide films in aluminum–calcium foamable alloys. Journal of Alloys and Compounds, 2016, 655, 433-441.	2.8	20
171	Synthesis and characterization of bipyridine cobalt( <scp>ii</scp> ) complex modified graphite screen printed electrode: an electrochemical sensor for simultaneous detection of acetaminophen and naproxen. RSC Advances, 2021, 11, 3049-3057.	1.7	20
172	Anti-icing performance on aluminum surfaces and proposed model for freezing time calculation. Scientific Reports, 2021, 11, 3641.	1.6	20
173	Novel Pt-Ag3PO4/CdS/Chitosan Nanocomposite with Enhanced Photocatalytic and Biological Activities. Nanomaterials, 2020, 10, 2320.	1.9	19
174	A novel spark plasma sintered TiC–ZrN–C composite with enhanced flexural strength. Ceramics International, 2020, 46, 29022-29032.	2.3	19
175	Grid-Connected Photovoltaic Systems with Single-Axis Sun Tracker: Case Study for Central Vietnam. Energies, 2020, 13, 1457.	1.6	19
176	Nano-construction of CuO nanorods decorated with g-C3N4 nanosheets (CuO/g-C3N4-NS) as a superb colloidal nanocatalyst for liquid phase C H conversion of aldehydes to amides. Journal of Molecular Liquids, 2021, 334, 116063.	2.3	19
177	Preparation of magnetic chitosan-supported palladium-5-amino-1H-tetrazole complex as a magnetically recyclable catalyst for Suzuki-Miyaura coupling reaction in green media. Journal of Molecular Structure, 2021, 1244, 130873.	1.8	19
178	Preparation of mesoporous TiO2-SiO2 by ultrasonic impregnation method and effect of its calcination temperature on photocatalytic activity. , 0, 92, 145.		19
179	Manufacturing ZrB2–SiC–TaC Composite: Potential Application for Aircraft Wing Assessed by Frequency Analysis through Finite Element Model. Materials, 2020, 13, 2213.	1.3	18
180	Advances in Designing Au Nanoparticles for Catalytic Epoxidation of Propylene with H2 and O2. Catalysts, 2020, 10, 442.	1.6	18

#	Article	IF	CITATIONS
181	Characterization of spark plasma sintered TiC–Si3N4 ceramics. International Journal of Refractory Metals and Hard Materials, 2021, 95, 105444.	1.7	18
182	A simple and sensitive approach for the electrochemical determination of amaranth by a Pd/GO nanomaterial-modified screen-printed electrode. RSC Advances, 2021, 11, 278-287.	1.7	18
183	Hydrothermal self - sacrificing growth of polymorphous MnO2 on magnetic porous - carbon (Fe3O4@Cg/MnO2): A sustainable nanostructured catalyst for activation of molecular oxygen. Molecular Catalysis, 2021, 509, 111603.	1.0	18
184	Metal organic framework-based nanostructure materials: applications for non-lithium ion battery electrodes. CrystEngComm, 2022, 24, 2925-2947.	1.3	18
185	Improved optical properties of YVO4:Eu3+ nano–layers on silica spheres. Materials Chemistry and Physics, 2018, 203, 274-279.	2.0	17
186	Recent Advances in the Electrochemical Sensing of Venlafaxine: An Antidepressant Drug and Environmental Contaminant. Sensors, 2020, 20, 3675.	2.1	17
187	Controlled growth and ion intercalation mechanism of monocrystalline niobium pentoxide nanotubes for advanced rechargeable aluminum-ion batteries. Nanoscale, 2020, 12, 12531-12540.	2.8	17
188	Fabrication of magnetic iron oxide-supported copper oxide nanoparticles (Fe3O4/CuO): modified screen-printed electrode for electrochemical studies and detection of desipramine. RSC Advances, 2020, 10, 15171-15178.	1.7	17
189	Copper(II) complex anchored on magnetic chitosan functionalized trichlorotriazine: An efficient heterogeneous catalyst for the synthesis of tetrazole derivatives. Colloids and Interface Science Communications, 2021, 44, 100471.	2.0	17
190	Applications of Nonâ€precious Transition Metal Oxide Nanoparticles in Electrochemistry. Electroanalysis, 2022, 34, 1065-1091.	1.5	17
191	Characteristics of dynamically-formed surface oxide layers on molten zinc–aluminum alloys: A multimodality approach. Thin Solid Films, 2018, 667, 34-39.	0.8	16
192	Effect of fuels on nanostructure and luminescence properties of combustion synthesized MgAl2O4:Eu3+ phosphors. Journal of Molecular Structure, 2019, 1193, 274-279.	1.8	16
193	Electrochemical activity of Samarium on starch-derived porous carbon: rechargeable Li- and Al-ion batteries. Nano Convergence, 2020, 7, 11.	6.3	16
194	Controllable growth and flexible optoelectronic devices of regularly-assembled Bi2S3 semiconductor nanowire bifurcated junctions and crosslinked networks. Nano Research, 2020, 13, 2226-2232.	5.8	16
195	BN-Fe3O4-Pd nanocomposite modified carbon paste electrode: Efficient voltammetric sensor for sulfamethoxazole. Ceramics International, 2021, 47, 13903-13911.	2.3	16
196	Hydroxyapatite Consolidated by Zirconia: Applications for Dental Implant. Journal of Composites and Compounds, 2019, 2, 26-34.	0.4	16
197	Optimal Separation of CO <sub>2</sub> /CH <sub>4</sub> /Brine with Amorphous Kerogen: A Thermodynamics and Kinetics Study. Journal of Physical Chemistry C, 2019, 123, 20877-20883.	1.5	15
198	Direct electrochemical detection of clozapine by RuO2 nanoparticles-modified screen-printed electrode. RSC Advances, 2020, 10, 13021-13028.	1.7	15

#	Article	IF	CITATIONS
199	Effect of Solvent on Nanostructure and Luminescence Properties of Combustion Synthesized Eu <sup>3</sup> <sup>+</sup> Doped Yttria. Nanoscience and Nanotechnology Letters, 2014, 6, 692-696.	0.4	15
200	Preparation and Characterization of Palladium Nanoparticles Supported on Nickel Hexacyanoferrate for Fuel Cell Application. Bulletin of the Korean Chemical Society, 2013, 34, 1195-1198.	1.0	15
201	Excellent adsorption of orange acid II on a water fern– derived micro- and mesoporous carbon. Journal of the Taiwan Institute of Chemical Engineers, 2019, 102, 99-109.	2.7	14
202	Adsorption based realistic molecular model of amorphous kerogen. RSC Advances, 2020, 10, 23312-23320.	1.7	14
203	Characterization of reactive spark plasma sintered (Zr,Ti)B2–ZrC–SiC composites. Journal of the Taiwan Institute of Chemical Engineers, 2021, 119, 187-195.	2.7	14
204	Chitosan supported 1-phenyl-1H-tetrazole-5-thiol ionic liquid copper(II) complex as an efficient catalyst for the synthesis of arylaminotetrazoles. Journal of Molecular Liquids, 2021, 341, 117398.	2.3	14
205	Synthesis and luminescence properties of transparent YVO <sub>4</sub> : Eu <sup>3+</sup> phosphors. Materials Research Express, 2018, 5, 116208.	0.8	13
206	Bentonite-supported furfural-based Schiff base palladium nanoparticles: an efficient catalyst in treatment of water/wastewater pollutants. Journal of Materials Science: Materials in Electronics, 2020, 31, 12856-12871.	1.1	13
207	A survey on spark plasma sinterability of CNT-added TiC ceramics. International Journal of Refractory Metals and Hard Materials, 2021, 96, 105471.	1.7	13
208	Functionalization of chitosan by grafting Cu(II)-5-amino-1H-tetrazole complex as a magnetically recyclable catalyst for C-N coupling reaction. Inorganic Chemistry Communication, 2022, 136, 109135.	1.8	13
209	Nanostructural approach to the thickening behavior and oxidation of calcium-stabilized aluminum foams. Materials Chemistry and Physics, 2018, 220, 351-359.	2.0	12
210	TEM characterization of hot-pressed ZrB2-SiC-AlN composites. Results in Physics, 2020, 19, 103348.	2.0	12
211	Preliminary Investigation of the Effects of Thermal Maturity on Redox-Sensitive Trace Metal Concentration in the Bakken Source Rock, North Dakota, USA. ACS Omega, 2020, 5, 7135-7148.	1.6	12
212	Iron molybdenum oxide-modified screen-printed electrode: Application for electrocatalytic oxidation of cabergoline. Microchemical Journal, 2020, 157, 104890.	2.3	12
213	Enhanced Luminescence Properties of Combustion Synthesized Y <sub>2</sub> O <sub>3</sub> :Gd Nanostructure. Current Nanoscience, 2016, 12, 244-249.	0.7	12
214	Template-free synthesis of porous boron nitride using a single source precursor. RSC Advances, 2015, 5, 46823-46828.	1.7	11
215	Decoration of metal oxide surface with {111} form Au nanoparticles using PEGylation. RSC Advances, 2018, 8, 18442-18450.	1.7	11
216	Phase transformation in spark plasma sintered ZrB2–V–C composites at different temperatures. Ceramics International, 2020, 46, 9415-9420.	2.3	11

#	Article	IF	CITATIONS
217	Cell cycle inhibition, apoptosis, and molecular docking studies of the novel anticancer bioactive 1,2,4-triazole derivatives. Structural Chemistry, 2020, 31, 691-699.	1.0	11
218	Sustainable design and novel synthesis of highly recyclable magnetic carbon containing aromatic sulfonic acid: Fe <sub>3</sub> O <sub>4</sub> @C/Ph—SO <sub>3</sub> H as green solid acid promoted regioselective synthesis of tetrazoloquinazolines. Applied Organometallic Chemistry, 2021, 35, e6346.	1.7	11
219	Bacterial vs. thermal degradation of algal matter: Analysis from a physicochemical perspective. International Journal of Coal Geology, 2020, 223, 103465.	1.9	10
220	Microstructural evolution of TiB2–SiC composites empowered with Si3N4, BN or TiN: A comparative study. Ceramics International, 2021, 47, 1002-1011.	2.3	10
221	Post hot rolling of spark plasma sintered Ti–Mo–B4C composites. Materials Science & Engineering A: Structural Materials: Properties, Microstructure and Processing, 2021, 799, 140214.	2.6	10
222	Microstructure–property correlation in nano-diamond and TiN added TiC-based ceramics. Ceramics International, 2021, 47, 449-460.	2.3	10
223	Characterization and FEA evaluation of a ZrB2–SiC ceramic containing TaC for beam–column joint application. Ceramics International, 2021, 47, 11438-11450.	2.3	10
224	Synergistic effects of Si3N4 and CNT on densification and properties of TiC ceramics. Ceramics International, 2021, 47, 12941-12950.	2.3	10
225	Architecture engineering of nanostructured catalyst via layer-by-layer adornment of multiple nanocatalysts on silica nanorod arrays for hydrogenation of nitroarenes. Scientific Reports, 2022, 12, 2.	1.6	10
226	Carbohydrate-based nanostructured catalysts: applications in organic transformations. Materials Today Chemistry, 2022, 24, 100869.	1.7	10
227	Heterogeneous Heck Reaction Catalyzed by Recyclable Polymer-SupportedN-Heterocyclic Carbene-Palladium Complex. Synlett, 2006, 2006, 0618-0620.	1.0	9
228	Effects of discrete and simultaneous addition of SiC and Si3N4 on microstructural development of TiB2 ceramics. Ceramics International, 2021, 47, 3520-3528.	2.3	9
229	Characterization of TiC ceramics with SiC and/or WC additives using electron microscopy and electron probe micro-analysis. Journal of the Taiwan Institute of Chemical Engineers, 2021, , .	2.7	9
230	Rendering Redox Reactions of Cathodes in Li-Ion Capacitors Enabled by Lanthanides. ACS Omega, 2020, 5, 1634-1639.	1.6	9
231	Modified chitosan-zeolite supported Pd nanoparticles: A reusable catalyst for the synthesis of 5-substituted-1H-tetrazoles from aryl halides. International Journal of Biological Macromolecules, 2022, 209, 1573-1585.	3.6	9
232	A novel ZrB2-based composite manufactured with Ti3AlC2 additive. Ceramics International, 2021, 47, 817-827.	2.3	8
233	Deformation, Cracking and Fracture Behavior of Dynamically-Formed Oxide Layers on Molten Metals. Metals and Materials International, 2021, 27, 1701-1712.	1.8	8
234	MEL zeolite nanosheet membranes for water purification: insights from molecular dynamics simulations. Journal of Nanostructure in Chemistry, 2022, 12, 291-305.	5.3	8

#	Article	IF	CITATIONS
235	Microstructure of spark plasma sintered TiC–TiB2–SiCw composite. Materials Chemistry and Physics, 2022, 281, 125877.	2.0	8
236	Backtracking to Parent Maceral from Produced Bitumen with Raman Spectroscopy. Minerals (Basel,) Tj ETQq0 (	) 0 rgBT /C	overlock 10 Tf
237	A TEM study on the microstructure of spark plasma sintered ZrB2-based composite with nano-sized SiC dopant. Progress in Natural Science: Materials International, 2021, 31, 47-54.	1.8	7
238	TGA and elemental analysis of type II kerogen from the Bakken supported by HRTEM. Journal of Natural Gas Science and Engineering, 2022, 103, 104606.	2.1	7
239	Magnetically recyclable nanocomposites via lanthanide-based MOFs grown on natural sea sponge: Screening hydrogenation of nitrophenol to aminophenol. Molecular Catalysis, 2022, 528, 112459.	1.0	7
240	Hollow ZnO microspheres self-assembled from rod-like nanostructures: morphology-dependent linear and Kerr-type nonlinear optical properties. Journal of Materials Science: Materials in Electronics, 2021, 32, 23385-23398.	1.1	6
241	Adsorption onto zeolites: molecular perspective. Chemical Papers, 2021, 75, 6217-6239.	1.0	6
242	ZrB2SiCw composites with different carbonaceous additives. International Journal of Refractory Metals and Hard Materials, 2021, 95, 105457.	1.7	5
243	2â€Dimensional Materials: Electrocatalytic Water Splitting and CO <sub>2</sub> Reduction: Sustainable Solutions via Singleâ€Atom Catalysts Supported on 2D Materials (Small Methods 9/2019). Small Methods, 2019, 3, 1970028.	4.6	4
244	Diffusivity and hydrophobic hydration of hydrocarbons in supercritical CO <sub>2</sub> and aqueous brine. RSC Advances, 2020, 10, 37938-37946.	1.7	3
245	Structural and optical characterizations of Ce 3+ â€doped YSO phosphors via the addition of TEOS. Luminescence, 2021, 36, 1117-1123.	1.5	2
246	Non-graphitizable resin coating on polyacrylonitrile-based polyHIPE to prepare high surface area graphitic carbon foam and the investigation of its electrochemical performance as an anode of lithium-ion batteries. Journal of Alloys and Compounds, 2021, 873, 159771.	2.8	2
247	HRTEM and XPS characterizations for probable formation of TiBxNy solid solution during sintering process of TiB2–20SiC–5Si3N4 composite. Materials Chemistry and Physics, 2022, 288, 126380.	2.0	2
248	Effect of iron nanoparticles on spark plasma sinterability of ZrB2-based ceramics. Journal of the Australian Ceramic Society, 0, , .	1.1	2